Carcinogenesis vol.33 no.5 pp.1098–1105, 2012
doi:10.1093/carcin/bgs122
Advance Access publication March 15, 2012

Evaluation of a mucoadhesive fenretinide patch for local intraoral delivery: a strategy to reintroduce fenretinide for oral cancer chemoprevention

Andrew S.Holpuch[1,*], Maynard P.Phelps[1], Kashappa-Goud H.Desai[2], Wei Chen[3,4], George M.Koutras[1], Byungdo B.Han[1], Blake M.Warner[1,5], Ping Pei[1], Garrett A.Seghi[1], Meng Tong[1], Michael B.Border[1], Henry W.Fields[6], Gary D.Stoner[7], Peter E.Larsen[1], Zhongfa Liu[3,8], Steven P.Schwendeman[2] and Susan R.Mallery[1,8]

[1]Division of Oral Maxillofacial Surgery, Pathology and Anesthesiology, College of Dentistry, The Ohio State University, 2205 Postle Hall, 305 W. 12th Avenue, Columbus, OH 43210-1241, USA, [2]Department of Pharmaceutical Sciences, University of Michigan, Ann Arbor, MI 48109, USA, [3]College of Pharmacy, The Ohio State University, Columbus, OH, USA, [4]Zhejiang Cancer Research Institute, Zhejiang Cancer Hospital, Hangzhou, Zhejiang 310022, China, [5]College of Public Health, The Ohio State University, Columbus, OH, USA, [6]Division of Orthodontics, College of Dentistry, The Ohio State University, Columbus, OH, USA, [7]Department of Medicine, Medical College of Wisconsin, Milwaukee, WI 53226, USA and [8]The Ohio State University Comprehensive Cancer Center, Columbus, OH, USA

[*]To whom correspondence should be addressed. Tel: +1 614 292 4028; Fax: +1 614 292 9384;
Email: holpuch.5@osu.edu

Systemic delivery of fenretinide in oral cancer chemoprevention trials has been largely unsuccessful due to dose-limiting toxicities and subtherapeutic intraoral drug levels. Local drug delivery, however, provides site-specific therapeutically relevant levels while minimizing systemic exposure. These studies evaluated the pharmacokinetic and growth-modulatory parameters of fenretinide mucoadhesive patch application on rabbit buccal mucosa. Fenretinide and blank-control patches were placed on right/left buccal mucosa, respectively, in eight rabbits (30 min, q.d., 10 days). No clinical or histological deleterious effects occurred. LC-MS/MS analyses of post-treatment samples revealed a delivery gradient with highest fenretinide levels achieved at the patch-mucosal interface (no metabolites), pharmacologically active levels in fenretinide-treated oral mucosa (mean: 5.65 μM; trace amounts of 4-oxo-4-HPR) and undetectable sera levels. Epithelial markers for cell proliferation (Ki-67), terminal differentiation (transglutaminase 1—TGase1) and glucuronidation (UDP-glucuronosyltransferase1A1—UGT1A1) exhibited fenretinide concentration-specific relationships (elevated TGase1 and UGT1A1 levels <5 μM, reduced Ki-67 indices >5μM) relative to blank-treated epithelium. All fenretinide-treated tissues showed significantly increased intraepithelial apoptosis (TUNEL) positivity, implying activation of intersecting apoptotic and differentiation pathways. Human oral mucosal correlative studies showed substantial interdonor variations in levels of the enzyme (cytochrome P450 3A4—CYP3A4) responsible for conversion of fenretinide to its highly active metabolite, 4-oxo-4-HPR. Complementary *in vitro* assays in human oral keratinocytes revealed fenretinide and 4-oxo-4-HPR's preferential suppression of DNA synthesis in dysplastic as opposed to normal oral keratinocytes. Collectively, these data showed that mucoadhesive patch-mediated fenretinide delivery is a viable strategy to reintroduce a compound known to induce keratinocyte differentiation to human oral cancer chemoprevention trials.

Abbreviations: BRB, black raspberry; HOK, human oral keratinocyte; IHC, immunohistochemistry; INMT, indolethylamine N-methyltransferase; PBS, phosphate buffered saline; TUNEL, terminal deoxynucleotidyl transferase-mediated dUTP nick end labeling.

Introduction

Over the past several decades, many promising cancer-preventing compounds have been evaluated in patients with oral premalignant lesions [reviewed in ref. (1)]. Systemic delivery trials that predominantly relied on oral capsule administration induced dose-limiting systemic toxicities and lacked initial and/or sustained efficacy (1). Formulations used in local delivery trials, e.g. mucoadhesive gels (2–4) and rinses, demonstrated a range of therapeutic efficacies largely without deleterious side effects (1). Notably, only 3 of the 19 reviewed trials (i.e. two local and one systemic) quantified compound levels achieved at the target site (1). This lack of data precludes determination of whether the compounds evaluated were pharmacologically ineffective or failed to reach therapeutic levels in lesional tissues (i.e. oral epithelium).

Many of these oral cancer chemopreventive studies evaluated vitamin A, its precursors and analogs (retinoids) (1). *In vitro*, fenretinide (a synthetic analog of all-*trans* retinoic acid) has shown exceptional capacity to promote keratinocyte terminal differentiation or apoptosis in a dose-dependent fashion (5). Furthermore, fenretinide exhibits a reduced toxicity–induction profile (i.e. decreased gastrointestinal distress and nyctalopia) and thus has been an agent of choice for recent oral cancer chemoprevention clinical trials (6–9). Fenretinide trials in patients with oral dysplastic lesions, however, have been largely unsuccessful (7–9). Notably, these studies investigated systemic delivery of fenretinide (oral capsule) at varying concentrations (low dose: 100 mg b.i.d. or 200 mg q.d., high dose: 900 mg b.i.d.), which resulted in minimal therapeutic efficacy accompanied by dose-limiting toxicities (7–9). Sera levels, which were used as a surrogate marker for target tissue levels, never achieved therapeutic concentrations (7–9). Issues such as first pass metabolism in the liver and reliance upon perfusion from the underlying vasculature to overlying target surface epithelium likely compromised intraoral levels achieved from systemic delivery. In contrast, a pilot local delivery trial in which patients placed fenretinide capsule contents on a variety of reactive and preneoplastic oral lesions did not demonstrate any local or systemic deleterious effects (10).

Our labs obtained promising results from a local delivery strategy that evaluated the effects of a 10% freeze-dried black raspberry (BRB) gel in patients with oral dysplastic lesions (2,3). Results from these and additional recent studies showed local gel delivery provided a pharmacologic advantage (4), a subset of patients responded favorably to local BRB gel application (2) and differential bioactivation and retention of chemopreventive compounds in human oral mucosa (11). These data, which implied that BRB was insufficient to induce regression in some patients' dysplastic oral lesions, served as the impetus for the current study. Considering these clinical implications, our laboratories recently developed a novel mucoadhesive patch, which provided improved site-specific intraoral delivery of fenretinide (12). The goal of the current study was to determine if mucoadhesive patches delivered therapeutically relevant fenretinide levels to oral mucosa. Subsequent evaluations of fenretinide-treated and blank-treated rabbit oral tissues assessed the modulation of chemopreventive and metabolic parameters. Corresponding studies of human oral tissues and cultured oral keratinocytes recapitulated the rabbit data and provided human clinical relevance.

Materials and methods

Intraoral mucoadhesive fenretinide patch pharmacokinetic analyses in New Zealand white rabbits

Rabbit studies were conducted with approval from the Ohio State University's Institutional Animal Care and Use Committee. Eight female New Zealand white rabbits (Harlan Laboratories, Indianapolis, IN) weighing 2.71 ± 0.18 kg

were used for analysis of intraoral fenretinide (a generous gift from Dr. Vernon Steele at the National Cancer Institute, Bethesda, MD) delivery from mucoadhesive patches (12). Upon arrival, rabbits were acclimated for 7 days and monitored for signs of distress. Following acclimation, each rabbit was sedated with a subcutaneous injection (0.2 cc) of acepromazine (2 mg/ml, Butler Schein Animal Health, Dublin, OH) and placed under general anesthesia via isoflurane inhalation (2–3 vol/vol%) for the entire 30 min patch application procedure. Once unconscious and prior to patch placement, 0.5 cc of blood was collected from the central ear artery. A fenretinide-loaded mucoadhesive patch [0.5 mg fenretinide/patch, i.e. 400- to 3600-fold less than daily systemic administrations in recent clinical trials (7–9)] was attached to the right buccal mucosa and a blank-control patch attached to the left buccal mucosa, both immediately posterior to the intraoral commissure of the upper and lower lips (Figure 1). Patches were left in place for 30 min and an additional blood sample collected at 30 min. The patches were then removed, fenretinide-treated underlying surface epithelium lavaged with 200 μl of 1× phosphate buffered saline (PBS) and patch–mucosa interface sample immediately collected. This procedure was conducted q.d. for 10 consecutive days.

Following treatment on day 10, rabbits were sacrificed via intravenous potassium chloride injection, and oral biopsies of the fenretinide-treated and blank-treated mucosal sites were harvested. Modulation of chemopreventive and metabolic parameters relative to intramucosal fenretinide concentrations was compared in intrarabbit blank-treated versus fenretinide-treated mucosal specimens, whereas patch-mucosal interface samples provided interrabbit comparisons of daily patch delivery efficacy. Notably, these oral biopsies were cut in two pieces: half for LC-MS/MS analysis (stored in stabilizing buffer: pH 6.5, 1× PBS + 9 mM ethylenediaminetetraacetic acid + 25 mM sodium ascorbate + 21 mM sodium sulfate) and the other half for protein analysis [half for immunohistochemistry (IHC): 10% formalin, half for western blot: RNA-Later]. All tissue and patch-mucosal interface LC-MS/MS samples were immediately frozen and stored at −80°C until analysis. Blood samples were clotted, centrifuged at 10 000*g*, serum supernatant collected and stored at −80°C until analysis.

Fig. 1. Mucoadhesive patch attachment on rabbit oral mucosa. Fenretinide mucoadhesive patches were attached (q.d., 30 min for 10 consecutive days) to the right buccal mucosa (blank patches on left buccal mucosa) immediately posterior to the intraoral commissure of the upper and lower lips. Pre- and posttreatment blood specimens and patch-mucosal interface samples were collected daily, and fenretinide-treated and blank-treated oral mucosal biopsies were harvested upon completion of the 10 day study. All samples were analyzed via LC-MS/MS to detect the levels of fenretinide and its metabolites (4-oxo-4-HPR and 4-MPR).

Preparation of rabbit patch-mucosal interface, oral mucosa homogenate and serum samples for LC-MS/MS analysis

Due to the high concentration of fenretinide present in the patch-mucosal interface samples, they were prediluted prior to analysis (i.e. serially diluted in 1× PBS 200- and 2000-fold). One-hundred micro liters of the 200- or 2000-fold diluted samples were mixed with 10 μl of internal standard (hesperetin, 10 μg/μl). Samples were extracted with 800 μl ethyl acetate for 30 min by mechanical shaking. For mucosa homogenate samples, both fenretinide and blank-treated samples were grossly dissected to remove excess amounts of underlying connective tissue. Oral epithelium was homogenized in 1× PBS for 3 × 5 min on a bead mill, and 260 μl of the homogenate was spiked with 10 μl of internal standard and 300 μl of lysis buffer. Samples were incubated on ice for 5 min, centrifuged at 11 000*g* for 1 min and the supernatant was extracted with 1 ml ethyl acetate for 30 min. To process rabbit serum samples, 100 μl of each rabbit serum sample was spiked with 10 μl of internal standard followed by extraction using 800 μl ethyl acetate for 30 min. After the extractions, all the samples were centrifuged at 11 000*g* for 1 min and ethyl acetate fraction was collected and evaporated to dryness under nitrogen stream. The residue was reconstituted in 100 μl of 50% methanol containing 0.2% formic acid and subsequently subjected to LC-MS/MS for analysis.

LC-MS/MS analysis

The LC-MS/MS analysis was conducted on a Thermo TSQ Quantum triple quadrupole mass spectrometer equipped with an electrospray ionization source, Shimadzu LC-20AD HPLC pump and LC-20AC autosampler. The samples were analyzed on a Thermo Betabasic C8 column (50 × 2.1 mm, 5 μm), of which the mobile phase (85% methanol with 0.2% formic acid) was used in isocratic mode with 0.2 ml/min flow rate. The analysis was conducted in positive mode. The transfer line temperature was 325°C. The multiple reaction monitoring transitions selected (based on parameters established by fenretinide/metabolite-spiked blank rabbit oral mucosal tissues and sera) for the analysis of fenretinide, 4-oxo-HPR, 4-MPR and the internal standard were 392 > 283, 406 > 297, 406 > 283 and 303 > 177 m/z, respectively.

Conversion of fenretinide mass quantities to molar equivalents

In order to compare oral mucosal fenretinide levels (ng fenretinide/gram tissue) to previously published therapeutic values (i.e. 1–10 μM), mass quantities were converted to micromolar concentrations, by standards previously published (13).

Evaluation and quantification of chemoprevention-associated markers and metabolic enzyme distribution within the rabbit surface epithelium by immunoblotting and immunohistochemical staining

The presence/absence of deleterious side effects within the fenretinide-treated and blank-treated rabbit oral mucosa was assessed by standard hematoxylin and eosin staining of paraffin-embedded tissues. Rabbit mucosal tissues were first screened by immunoblotting to determine the presence or absence of proteins associated with or responsive to fenretinide. Matched rabbit oral mucosal specimens were also analyzed by IHC to elucidate levels of immunoblot-confirmed metabolic enzymes and chemopreventive endpoints within the target oral epithelia. The antibodies employed for western blot and IHC staining were: goat polyclonal UGT1A1 (WB: 1:100, IHC: 1:300), goat polyclonal UGT1A6 (WB: 1:100, IHC: not conducted), mouse monoclonal CYP3A4 (WB: 1:250, IHC: not conducted), mouse monoclonal CYP26A1 (WB: 1:250, IHC: not conducted), goat polyclonal CYP2C8/9/18/19 (WB: 1:500, IHC: not conducted), mouse monoclonal Ki-67 (WB: not conducted—highly specific in IHC applications (14), IHC: 1:150), mouse monoclonal keratinocyte-specific transglutaminase 1 (TGase 1; WB: 1:100, IHC: 1:50 and 1:300) antibodies (Santa Cruz Biotechnology, Santa Cruz, CA). Blocking buffer (negative control) was used in place of the primary antibody, and all tissue sections (including negative control) were incubated with their respective biotinylated secondary antibody (1:200; Vector Laboratories, Burlingame, CA). Vectastain ABC reagent (Vector Laboratories) was applied, and identically timed immunoreactions were conducted with diaminobenzidene substrate and hematoxylin counterstain. Evaluation of apoptotic indices in fenretinide-treated versus blank-treated rabbit epithelium was assessed via an immunofluorescent terminal deoxynucleotidyl transferase-mediated dUTP nick end labeling (TUNEL) assay (Roche Diagnostics, Indianapolis, IN). Immunohistochemical and immunofluorescent images were obtained with identical magnification and exposure limits using a Nikon DS-Fi-1 high-resolution digital camera and analyzed via Image-Pro Plus 6.2 software (Media Cybernetics, Bethesda, MD).

Image analysis and quantification was conducted on the positive reacted antibodies: Ki-67, TGase 1, TUNEL and UGT1A1 tissue sections. Quantification of positive Ki-67 nuclear staining was conducted by selecting the basal epithelial layer of cells as the area of interest, setting limits of staining intensity

considered to be positive (identical for intrarabbit tissues) and quantifying the positive nuclear indices relative to basement membrane length (i.e. Ki-67 positive nuclei/length of epithelial basement membrane). Similarly, quantification of the TGase 1, TUNEL and UGT1A1 tissue specimens involved selection of the positive staining intensity limits (identical for intrarabbit tissues) within the area of interest (i.e. entire oral epithelium excluding the non-staining superficial orthokeratin layer) and quantification by area of positive staining relative to total epithelial area of interest. Notably, these methods of IHC quantification are restrictive to intrarabbit comparisons (i.e. interrabbit comparisons are not appropriate due to variation of the selected interrabbit positivity limits).

Evaluation of metabolic enzyme heterogeneity in human oral mucosa by western blot

Eight clinically and histologically normal human oral mucosal tissues were collected from patients undergoing elective oral surgical procedures. Human subject participation was approved by Ohio State University's Institutional Review Board and followed the tenets of the Declaration of Helsinki 1964. Tissues were collected and immediately bisected for western blot (mammalian protein extraction reagent; subsequent homogenization, protein extraction and Bradford protein quantification) or immunohistochemical (10% formalin; subsequent standard tissue processing) analyses. Western blot analyses were conducted using the iBlot western blot system (Invitrogen, Carlsbad, CA) on 4–12% Bis-Tris gels (Invitrogen). Thirty micrograms of human oral mucosal protein were loaded in each well, pooled human liver microsomes (BD Biosciences, San Jose, CA) were loaded as a positive control, separated by sodium dodecyl sulfate–polyacrylamide gel electrophoresis and blotted by the standard iBlot protocol (i.e. nitrocellulose stacks and 7 min transfer time). Blots were incubated in 5% non-fat milk blocking buffer overnight at 4°C with the following primary antibodies: CYP3A4 (1:250), CYP26A1 (1:250), CYP2C8 (1:500), UGT1A1 (1:250), UGT1A6 (1:250), indolethylamine N-methyltransferase (rabbit polyclonal; INMT, 1:1000; Sigma–Aldrich, St Louis, MO) and beta-actin loading control (1:20 000, Santa Cruz). Each blot was subsequently incubated at room temperature for 1 h with the respective horseradish peroxidase secondary antibody: goat anti-mouse, goat anti-rabbit or donkey anti-goat (1:1000, Santa Cruz) in blocking buffer. Following secondary antibody, incubation blots were incubated with the ECL Plus western blot detection system (Amersham GE Healthcare Life Sciences, Buckinghamshire, UK) and exposed on CL-Xposure films (Kodak, Rochester, NY). Quantification of positive immunoreactive bands (i.e. CYP3A4) was assessed via densitometry analysis (Kodak 1D3 image analysis software; Kodak) and results normalized relative to the expression of endogenous β-actin.

Determination of site specificity of metabolic enzymes in human oral mucosa by immunohistochemical analyses

Although western blots demonstrate relative levels of the protein of interest within the full-thickness oral mucosa specimens, they do not specify relative levels of tissue distribution in the targeted treatment site, i.e. oral epithelium. To identify the site-specific distribution of protein levels in oral mucosa, immunohistochemical analyses were therefore conducted for CYP3A4 (1:100) by the methods described previously.

Assessment of cell proliferation following fenretinide and 4-oxo-4-HPR treatments of human oral keratinocytes in vitro

Normal human oral keratinocytes (HOK) were cultured in oral keratinocyte growth medium with oral keratinocyte growth supplement and penicillin/streptomycin (ScienCell, Carlsbad, CA). A dysplastic cell strain was developed through stable transduction of the human papillomavirus E6/E7 genes in the HOKs, as per previously published methods (15). HOK E6/E7 transduction was confirmed via PCR and western blot (data not shown).

Evaluation of the effects of fenretinide (4-HPR) and its bioactive metabolite 4-oxo-4-HPR on cell proliferation was conducted using the BrdU cell proliferation ELISA (Roche). Briefly, log growth HOK or HOK E6/E7 cells were seeded at 1×10^4 cells per well in 24-well plates. Cells were treated daily with vehicle (0.01% dimethyl sulfoxide), 1, 5 or 10 μM 4-HPR or 4-oxo-4-HPR for 24, 48 and 72 h time points. BrdU (10 μM) was added 24 h prior to the respective cell harvesting time point, where subsequent detection (absorbance: 370 nm) of BrdU incorporation followed the standard protocol (Roche) on a FLUOstar Omega plate reader (BMG Labtech, Cary, NC).

Statistical analysis

Normality of data was assessed using the Shapiro–Wilks test to determine the appropriate use of parametric or non-parametric statistical tests. Fenretinide-treated versus blank-treated rabbit mucosal specimens were compared using the Wilcoxon matched-pairs signed-ranks test. Interrabbit variations of mean 10 day fenretinide levels at the patch-mucosal interface were evaluated with the Kruskal–Wallis non-parametric analysis of variance. Fenretinide-treated and blank-treated immunohistochemical sections were compared using the Wilcoxon matched-pairs signed-ranks test (TGase 1 and Ki-67) and paired *t*-test (TUNEL and UGT1A1). BrdU incorporation in HOK and HOK E6/E7 cells following 4-HPR and 4-oxo-4-HPR treatment was evaluated using a Kruskal–Wallis non-parametric analysis of variance followed by a Dunn's multiple comparisons posttest.

Results

Therapeutically relevant fenretinide levels are achieved in rabbit oral mucosa without deleterious side effects

Intraoral fenretinide mucoadhesive patch application delivered a fenretinide gradient with the highest levels achieved at the patch-mucosal interface, pharmacologically active levels in treated oral mucosa and undetectable sera levels (Figure 2A). Levels of fenretinide achieved at the fenretinide-treated patch-mucosal interface (mean ± SEM: 11513.9 ± 391.2 ng/mg protein) were comparable in all animals throughout the 10 day treatment period ($P > 0.5$, $n = 8$). Furthermore, levels in fenretinide-treated oral mucosa were significantly greater than their rabbit-matched blank-treated sites [fenretinide-treated mean ± SEM: 2210.3 ± 986.2 ng/gm tissue (5.65 ± 2.52 μM) versus blank-treated mean ± SEM: 9.0 ± 0.08 ng/gm tissue (0.02 ± 0.00 μM), $P < 0.01$, $n = 8$]. Despite achieving intramucosal fenretinide concentrations greater than the *in vitro*-established therapeutic range (i.e. 1–10 μM) in rabbits VII (12.98 μM) and VIII (19.96 μM) and the presence of a natural fenretinide reservoir, i.e. buccal fat pad, both clinical and histopathological assessments of treatment sites revealed normal oral mucosa; Figure 2B. In addition, the inactive fenretinide metabolite 4-MPR was not detected in the patch-mucosal interface, oral mucosa or serum samples, whereas trace amounts (i.e. below the linear level of quantification) of 4-oxo-4-HPR were observed in the fenretinide-treated oral mucosal samples of rabbits III through VIII.

Fenretinide modulates oral epithelial growth state parameters

Immunohistochemical analyses of fenretinide-treated tissue relative to matched blank-treated tissue exhibited fenretinide concentration-dependent patterns with regard to cell proliferation (Ki-67), terminal differentiation (TGase 1) and apoptosis (TUNEL). Although the Ki-67 findings were not statistically significant, moderate decreases in cell proliferation were observed in oral mucosal tissues containing >5 μM fenretinide (i.e. rabbits VII and VIII; Figure 3A and B). Similarly, TGase 1 levels were increased in oral mucosal tissues with levels of fenretinide in the range of 0.1–5 μM (i.e. rabbits I–VI), whereas TGase 1 levels were decreased in tissues containing >5 μM (i.e. rabbits VII and VIII; Figure 3A). This relationship was further demonstrated in the representative photomicrographs in Figure 3B, in which rabbit IV (2.22 μM) exhibited a 54.0% increase of TGase 1 levels in the fenretinide-treated relative to the blank-treated epithelium and rabbit VIII (19.96 μM) exhibited a 24.0% decrease of TGase 1 levels in the fenretinide-treated relative to blank-treated epithelium. Notably, the TGase 1 staining pattern in rabbit IV (differentiation-inducing levels) extended from the basal to the granular layers and was strongest in the keratinocyte cytosol. In contrast, the fenretinide-treated tissue from rabbit VIII (apoptosis-inducing levels) exhibited strong nuclear staining in the basal layer, which also extended to the spinous and granular layers. Furthermore, all of the fenretinide-treated oral epithelial tissues showed significantly increased apoptotic indices (Figure 3A; $P < 0.01$), which tended to be elevated in tissues with >3 μM fenretinide, as demonstrated in Figure 3B. Notably, inset photomicrographs in Figure 3B represent positive indices (red highlighted areas—Ki-67 and TGase 1) or negative control (TUNEL—due to inherent auto-fluorescence in paraffin-embedded tissue sections).

Induction of UGT1A1 levels in fenretinide-treated rabbit oral epithelium

Immunohistochemical analysis of fenretinide-related phase I/II metabolic enzymes identified significantly increased UGT1A1 expression

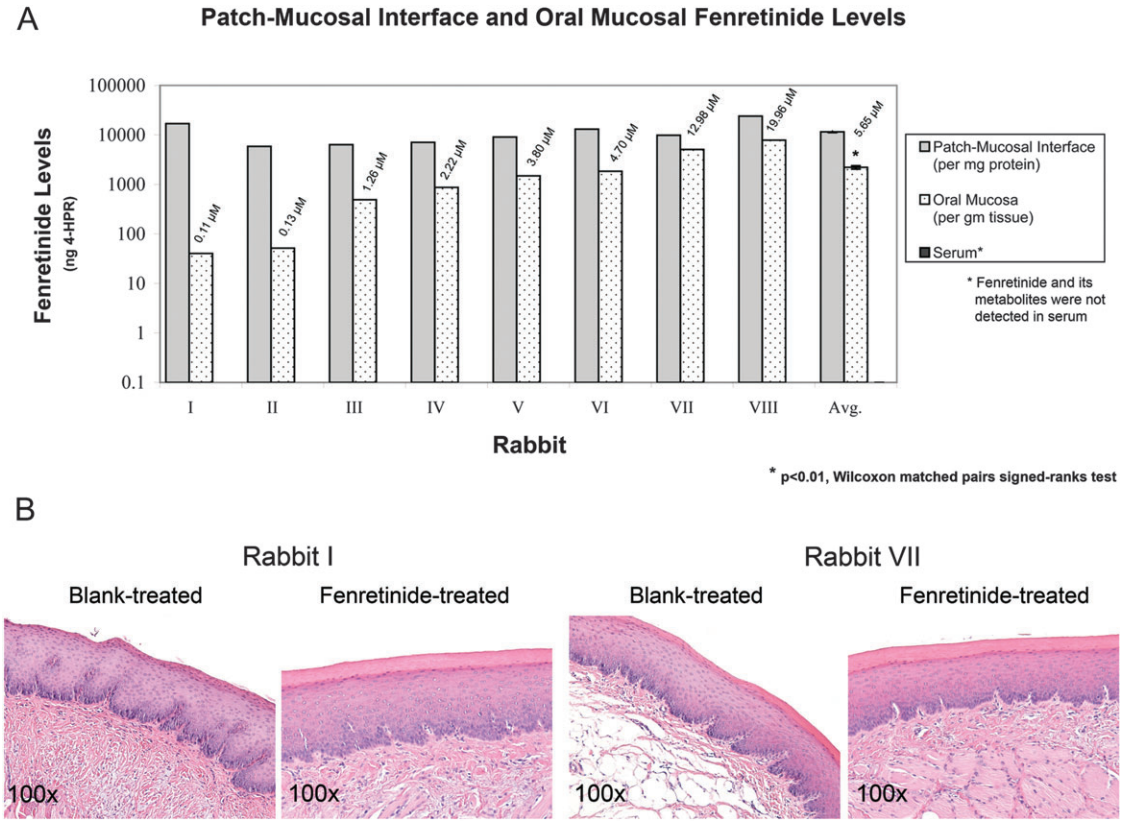

Fig. 2. Intraoral fenretinide patch application delivered pharmacological intraoral levels and did not induce any deleterious side effects. (**A**) Patch application delivered a fenretinide gradient with highest levels achieved at the patch-mucosal interface, therapeutically relevant levels in the treated oral mucosa (mean ± SEM: 5.65 ± 2.52 μM, $n = 8$) and undetectable levels in sera (linear limit of quantification: 1 ng/ml analyte). (**B**) Histopathological evaluation of hematoxylin and eosin-stained blank-treated and fenretinide-treated rabbit tissues revealed histologically normal oral mucosa. No evidence of either intraepithelial or superficial connective tissue contact mucositis or inflammation was observed.

in fenretinide-treated relative to blank-treated rabbit oral mucosal tissues ($P < 0.01$; Figure 4B). Notably, the percent of UGT1A1 induction was greatest in the mucosal samples with <5 μM fenretinide (i.e. rabbit I-VI; Figure 4B). Representative photomicrographs demonstrated a dose-dependent effect of fenretinide on phase II enzyme induction (Figure 4C). Additional fenretinide-specific metabolic enzymes (i.e. CYP3A4, CYP2C8, CYP26A1 and INMT) were not detected in rabbit oral mucosa (data not shown).

Human oral mucosa contained fenretinide-related metabolic enzymes capable of generating the bioactive 4-oxo-4-HPR metabolite and also exhibits appreciable interindividual heterogeneity

In contrast to rabbit oral mucosa, human oral epithelia possessed CYP3A4 (Figure 5). As demonstrated by immunoblotting, considerable interpatient heterogeneity of protein levels was exhibited (i.e. 16-fold difference of CYP3A4 in samples 2 and 5; Figure 5). These levels of protein expression were not associated with the amount of epithelium in each sample and, therefore, reflected actual interpatient variations. In addition, the fenretinide-related metabolic enzymes CYP2C8, CYP26A1 and INMT were not detected in human oral mucosa, whereas results from UGT1A1 and UGT1A6 immunoblots were inconclusive (data not shown).

Fenretinide and its bioactive metabolite 4-oxo-4-HPR modulated the growth state of cultured normal HOK

Evaluation of 4-HPR and its oxidized bioactive metabolite 4-oxo-4-HPR treatment effects on BrdU incorporation in normal and dysplastic oral keratinocytes showed a preferential suppression of DNA synthesis in dysplastic as opposed to normal keratinocytes. Dose, duration and treatment compound all impacted BrdU incorporation ($P < 0.05$; Figure 6). Although 4-HPR treatment did not significantly decrease DNA synthesis in dysplastic relative to normal cells at 24 h, subsequent 48 and 72 h time points showed significant inhibition in the 5 μM treated oral dysplastic cells ($P < 0.05$). 4-oxo-4-HPR treatment resulted in significantly decreased BrdU incorporation in dysplastic cells relative to normal at all time points (24 h: 10 μM, 48 h: 10 μM, 72 h: 5 μM; $P < 0.05$).

Discussion

Despite its favorable chemopreventive profile *in vitro*, systemic administration of fenretinide in oral cancer chemoprevention clinical trials has demonstrated limited therapeutic efficacy and dose-limiting side effects (7–9). In contrast, local delivery strategies can circumvent first pass liver metabolism, minimize systemic exposure and deliver therapeutically relevant drug levels to the target tissues. Location, however, is paramount when considering use of local delivery formulations. The oral cavity is an optimal site for local delivery as it is amenable to direct visualization, which facilitates both agent placement and clinical monitoring. The basis for this current study arose from our familiarity with local delivery formulations in conjunction with our enthusiasm to reintroduce fenretinide for clinical oral cancer chemoprevention trials.

These pharmacokinetic studies confirmed the therapeutic advantage imparted by intraoral fenretinide mucoadhesive patch application, i.e. delivery of pharmacologically active levels of fenretinide to the rabbit oral mucosa (i.e. 5.65 μM average) while negating systemic exposure and toxicities. Our data also showed undetectable levels of the inactive metabolite 4-MPR and trace amounts of the potent

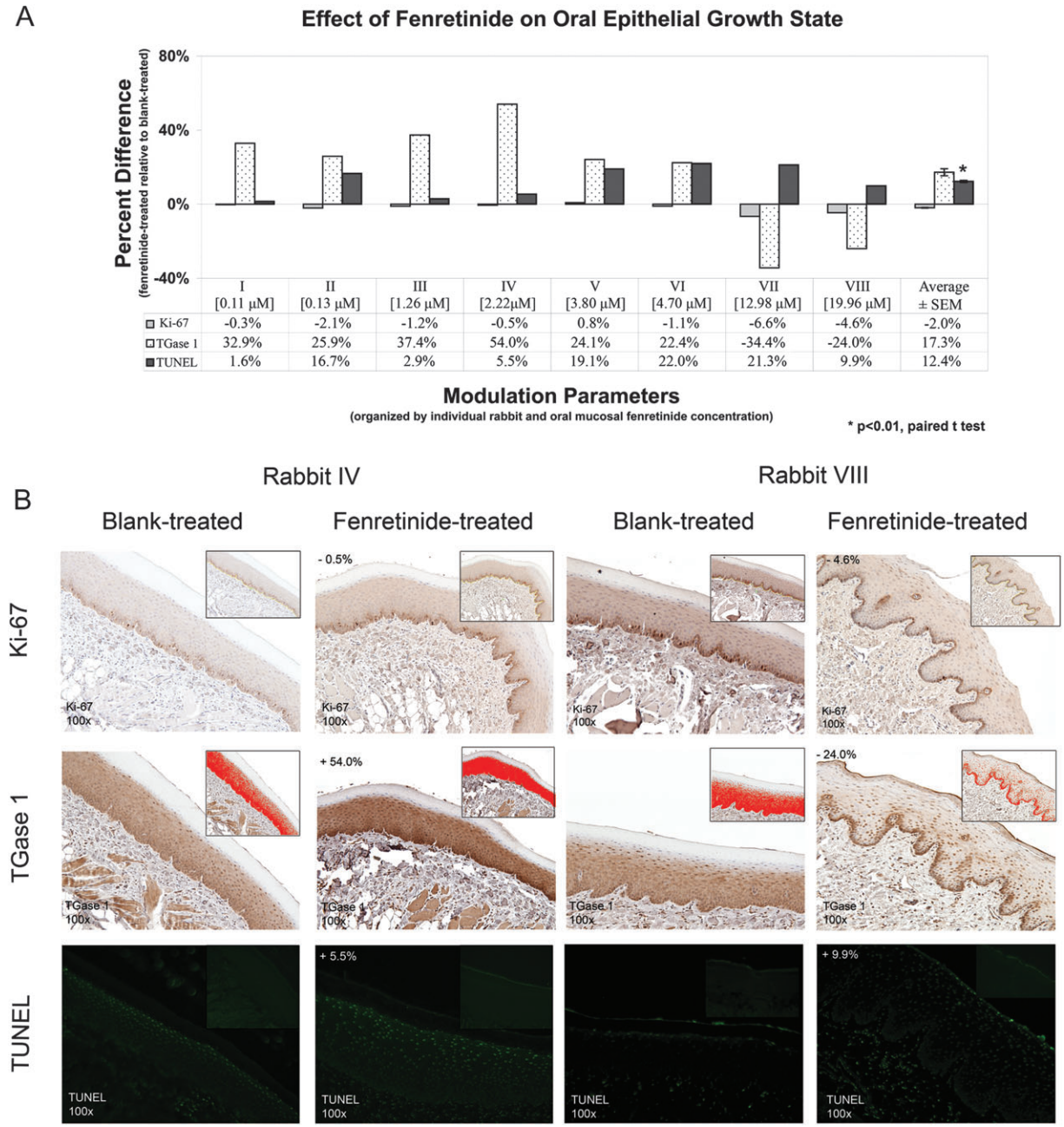

	I [0.11 μM]	II [0.13 μM]	III [1.26 μM]	IV [2.22μM]	V [3.80 μM]	VI [4.70 μM]	VII [12.98 μM]	VIII [19.96 μM]	Average ± SEM
Ki-67	-0.3%	-2.1%	-1.2%	-0.5%	0.8%	-1.1%	-6.6%	-4.6%	-2.0%
TGase 1	32.9%	25.9%	37.4%	54.0%	24.1%	22.4%	-34.4%	-24.0%	17.3%
TUNEL	1.6%	16.7%	2.9%	5.5%	19.1%	22.0%	21.3%	9.9%	12.4%

Fig. 3. Quantified immunohistochemical analyses showed fenretinide's dose-specific effects on treated rabbit oral epithelia growth state. (**A**) Results of these studies showed that lower fenretinide levels (<5 μM) elicited differentiation effects. While Ki-67 positivity was modestly reduced in epithelia of rabbits I through VI (<5 μM), epithelial proliferation was markedly decreased at higher fenretinide levels (>5 μM, rabbits VII and VIII). Similarly, TGase 1 levels (indicator of terminal differentiation) showed higher induction at lower fenretinide levels (<5 μM). Apoptosis (TUNEL indices) was significantly increased in fenretinide-treated relative to blank-treated mucosal epithelia ($n = 8$). These data, however, did not demonstrate an apparent dose-dependent relationship. (**B**) IHC images were quantified (blank-treated relative to fenretinide-treated epithelia) by designating the stratum basale (Ki-67) or full-thickness epithelia (excluding orthokeratinized layer—TGase 1 and TUNEL) as the area of interest. Positive indices (denoted by red highlighted areas in the inset photomicrographs—Ki-67 and TGase 1) were divided by the total area of interest (TGase 1 and TUNEL) or by the basement membrane length (Ki-67; yellow line in the inset photomicrograph).

metabolite 4-oxo-4-HPR in the fenretinide-treated rabbit oral mucosal samples. Accompanying western blots did not show the presence of the major metabolic enzymes responsible for conversion of fenretinide to 4-MPR (amine N-methyltransferases, such as INMT) or 4-oxo-4-HPR (CYP3A4, CYP2C8, CYP26A1) in rabbit oral mucosa (16,17). The trace amount of 4-oxo-4-HPR detected could therefore reflect 4-HPR metabolism by other cytochrome P450 enzymes or oral microflora. While technical challenges prevented LC-MS/MS detection of 4-HPR-O-glucuronide, the marked induction of UGT1A1 levels in rabbits I through VI suggested concomitant fenretinide metabolism to the more potent 4-HPR-O-glucuronide (18). This finding was limited to the percent increase relative to the blank-treated control tissues (i.e. not total epithelial levels of UGT1A1), and therefore assumed increased metabolism with enzyme induction. Notably, the marked induction of UGT1A1 in rabbits I through VI was coupled with low-baseline enzyme levels in the blank-treated control tissues, whereas rabbits VII and VIII demonstrated elevated baseline levels and minimal induction. Similar to previous studies demonstrating maximal phase II enzyme expression (19), these findings also suggested that UGT1A1 is maximally expressed in rabbits VII and VIII.

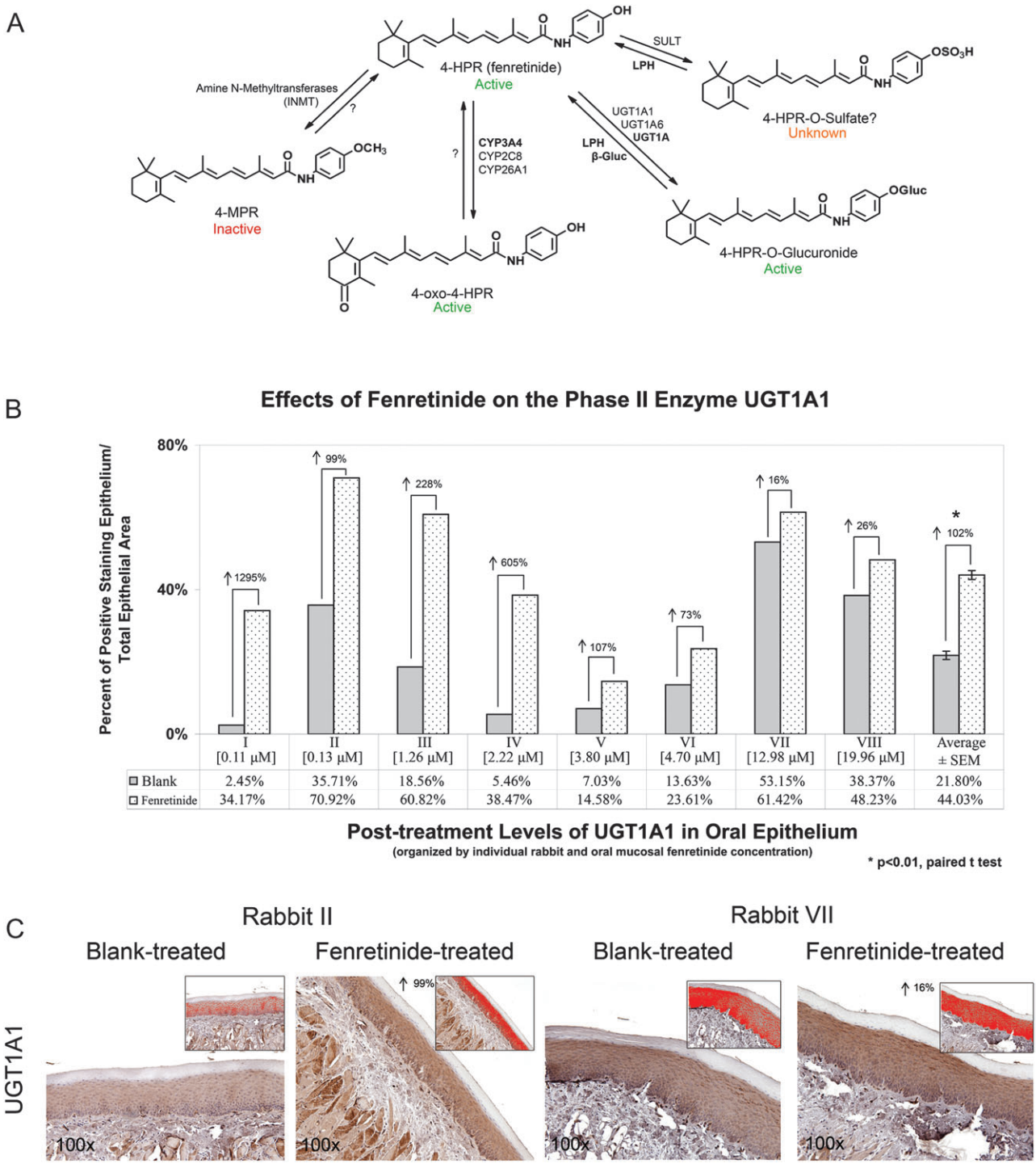

Fig. 4. Patch-delivered fenretinide effects intraepithelial metabolic enzyme profile. (**A**) Human oral mucosa fenretinide metabolic pathways can include generation of the inactive metabolite (4-MPR), active metabolites (4-oxo-4-HPR and 4-HPR-O-glucuronide) and the functionally unknown metabolite (4-HPR-O-sulfate). Pathways that can contribute to local oral recycling of metabolites back to the parent compound are similarly indicated. Abbreviations and intraoral locations are as follows: LPH, lactase phlorizin hydrolase (oral microflora); β-gluc, β-glucuronidase (human saliva); SULT, sulfotransferase (absent in human oral cavity); UGT1A, UDP-glucuronosyltransferase 1A (human oral epithelium); CYP3A4, cytochrome P450 3A4 (human oral epithelium); INMT, indolethylamine N-methyltransferase (absent in human oral cavity). (**B**) Differentiation-inducing levels of fenretinide (<5 µM) increased intraepithelial levels of UGT1A1 relative to blank-treated tissues. (**C**) Positive staining in the red highlighted area (area of interest) was used to quantify UGT1A1 levels.

Also, observed in these studies was a delivery gradient, in which highest fenretinide levels were consistently achieved at the patch-mucosal interface, followed by second highest, variable levels within the targeted epithelium. Ideally, highest fenretinide levels should be achieved at the pivotal basal layer cells that direct keratinocyte growth and differentiation. The constant interrabbit levels at the patch-mucosal interface suggested effective patch delivery while the range of intramucosal fenretinide concentrations was likely attributed to interrabbit epithelial permeability variations. This permeability issue was addressed in a recent study by our laboratories, which evaluated a fenretinide mucoadhesive patch formulated with the permeability enhancers propylene glycol and menthol (20). This

permeability-enhanced patch demonstrated consistent fenretinide penetration of rabbit oral mucosa following a single 30 min patch application, which achieved comparable intramucosal levels to those observed in the current 10 day study (20). Furthermore, these collective findings (i.e. similar intramucosal fenretinide levels after a single 30 min patch application and 30 min application q.d. for 10 days) suggested that therapeutic levels of fenretinide were achieved after each 30 min patch application and were subsequently metabolized and cleared from the treatment site prior to subsequent patch application 24 h later. Similarly, these observations indicated that transient fenretinide levels affect keratinocyte protein translation in a therapeutic fashion.

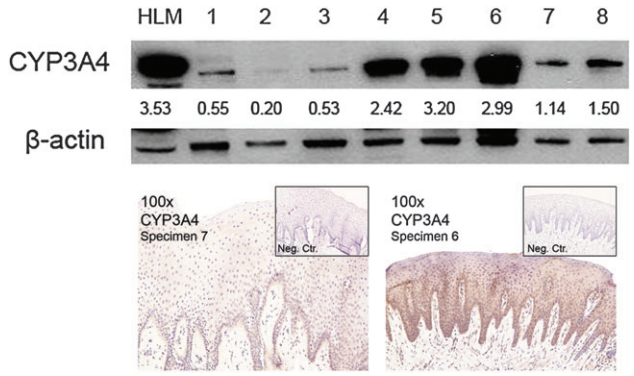

Fig. 5. Immunoblots of normal human oral mucosa revealed considerable interdonor heterogeneity in a fenretinide bioactivating enzyme, CYP3A4. Similar to other intraepithelial metabolic enzymes, CYP3A4 was primarily distributed in the lower epithelial layers (i.e. basilar and spinous), with decreased levels in the increasingly differentiated granular and cornified layers. Notably, levels of additional fenretinide-activating enzymes (i.e. CYP2C8 and CYP26A1) and the fenretinide-inactivating/eliminating enzyme (i.e. INMT) were not detected in the human oral epithelia. Although previous studies have demonstrated the presence of UGT1A enzymes in human oral epithelia (11), UGT1A1 and UGT1A6 immunoblots were indeterminate (data not shown).

A distinct rabbit versus human species variation was seen with regard to oral mucosal tissues' fenretinide metabolic profile. The present and previous studies by our laboratory confirm the presence of highly variable levels of UGT1A and CYP3A4 enzymes in normal human oral epithelium, implying the probable metabolism of fenretinide to its active metabolites 4-HPR-O-glucuronide and 4-oxo-4-HPR in human applications (11). Additionally, while the absence of INMT in human oral mucosa suggests the inability to form the inactive metabolite 4-MPR, other members of the amine N-methyltransferase family could also inactivate fenretinide (16). Collectively, the human fenretinide-related metabolic enzyme profile favors production of bioactive metabolites and exhibits the capacity for increased fenretinide retention at the treatment site via local enteric recycling (i.e. 4-HPR-O-glucuronide recycling by bacterial β-glucuronidases (11)). The large interpatient heterogeneity, however, will probably necessitate individual metabolic enzyme profiling to determine optimal duration and frequency of patch placement to achieve the desired therapeutic effect (i.e. patients with an elevated metabolic capacity could benefit from multiple doses throughout the day to effectively increase the drug levels at the target site).

The observed dose-dependent modulation of the keratinocyte growth state recapitulated previously published *in vitro* differentiation-associated concentrations and also confirmed that patch-delivered fenretinide retained its bioactive properties (5). Although not statistically significant, levels of the enzyme responsible for cornified envelope formation, i.e. TGase 1, increased in all oral mucosa tissues containing 0.1–5 μM fenretinide (i.e. previously established differentiation range). In contrast, tissues with fenretinide levels >10 μM (i.e. apoptotic range (5)) contained reduced TGase 1 levels. Interestingly, apoptotic indices were not drastically increased in the oral tissues with >10 μM fenretinide and did not inversely correlate with the TGase 1 data. These preliminary findings could reflect the complexity and interaction of the pathways responsible for the keratinocyte transitioning from a proliferative growth state. These somewhat paradoxical results are supported by the concept that epithelial differentiation is a specialized form of apoptosis (21,22) and, key to the chemopreventive aspect, both pathways result in the keratinocyte leaving the proliferative pool. Furthermore, several studies have shown nuclear translocation of the other transglutaminase

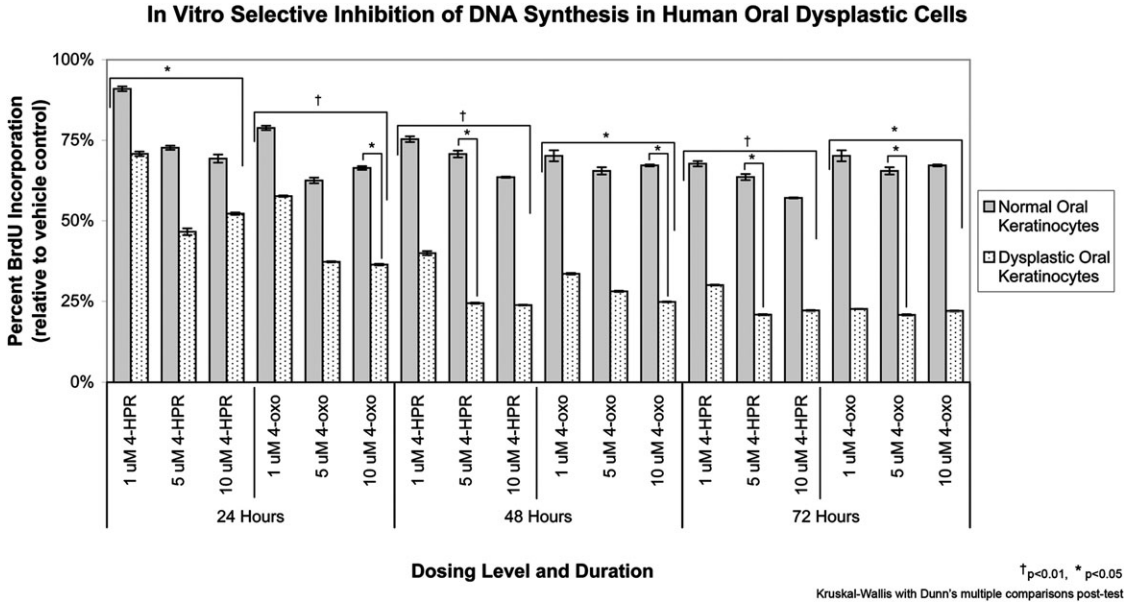

Fig. 6. Fenretinide and its bioactive metabolite 4-oxo-4-HPR demonstrated preferential growth suppression toward premalignant (dysplastic) oral keratinocytes. Treatment of normal and dysplastic oral keratinocytes with doses of fenretinide or 4-oxo-4-HPR that are achievable via mucoadhesive patch delivery significantly decreased DNA synthesis in a dose, cell strain and time-dependent fashion. Dysplastic keratinocytes were markedly more susceptible to suppression of DNA synthesis. These data convey the promise for mucoadhesive fenretinide patch application in oral cancer chemoprevention.

isoform (TGase 2) resulted in cross-linking of transcription factors and subsequent induction of apoptosis (23,24). Although the relationship between TGase 1 nuclear staining and TUNEL positivity was not definitive, the prospect that TGase 1 fulfills a similar role in keratinocytes is highly probable. Ongoing studies in our labs are investigating these interactions.

Our data show that the Ki-67 proliferation indices in normal rabbit oral epithelia were not affected by fenretinide patch application. As preservation of an intact oral mucosal surface is essential for defense, these findings are favorable. Similarly, normal oral keratinocyte proliferation, as assessed by BrdU incorporation, was not perturbed by the addition of either fenretinide or 4-oxo-4-HPR. Treatment of dysplastic oral keratinocytes, however, showed both fenretinide and 4-oxo-4-HPR significantly suppressed DNA synthesis; suggesting the prospect for preferential targeting of dysplastic relative to normal keratinocytes. Similarly, if future studies demonstrate that 4-oxo-4-HPR provides greater therapeutic efficacy than fenretinide, subsequent patch formulations would deliver the bioactive metabolite, 4-oxo-4-HPR.

Lesions of oral epithelial dysplasia are molecularly and biochemically diverse (25). It is therefore reasonable to predict that combinations as opposed to a single category agent may be necessary for chemoprevention of some dysplastic lesions. Indeed, our previous BRB gel chemoprevention trial, in which a subset of patients' lesions did not respond to topical gel application, emphasizes this point. In addition, complimentary local delivery strategies (e.g. mucoadhesive patch and rinse) would provide both site-specific and field coverage components to aid in the prevention of initial and second primary oral dysplastic lesions. A locally deliverable fenretinide formulation reintroduces a potent keratinocyte differentiation-inducing agent to the oral chemoprevention battery and initiates the prospect for anthocyanin–retinoid-based combination therapy.

Funding

National Institute of Health's National Cancer Institute (R01 CA129609, RC2 CA148099, R21 CA132138 to S.R.M.); National Institute of Dental and Craniofacial Research (F30 DE020992 and T32 DE14320 to A.S.H.) and National Heart, Lung, and Blood Institute (R01 HL68345 to S.P.S.). Additional funding was provided by the Fanconi Anemia Research Fund and National Center for Research Resources (UL1RR025755) to S.R.M.; Pelotonia Fellowship Program (to G.M.K.; any opinions, findings and conclusions expressed in this material are those of the authors and do not necessarily reflect those of the Pelotonia Fellowship Program); the American Association for Dental Research Student Research Fellowship (to A.S.H.) and the Ohio Division of the American Cancer Society Fellowship (to M.P.P.).

Acknowledgements

The authors wish to thank Dr. Vernon Steele from the National Institute of Health's National Cancer Institute for generously providing the fenretinide used in these studies. In addition, the authors thank Mary Lloyd and Mary Marin for their assistance with tissue processing and Drs Laura Gallaugher and Michelle Creamer for providing expert advice throughout the rabbit studies.

Conflict of Interest Statement: None declared.

References

1. Holpuch,A.S. *et al*. (2011) Optimizing therapeutic efficacy of chemopreventive agents: a critical review of delivery strategies in oral cancer chemoprevention clinical trials. *J. Carcinog.*, **10**, 23.
2. Mallery,S.R. *et al*. (2008) Topical application of bioadhesive black raspberry gel modulates gene expression and reduces cyclooxygenase 2 protein in human premalignant oral lesions. *Cancer Res.*, **68**, 4945–4957.
3. Shumway,B.S. *et al*. (2008) Effects of topically applied bioadhesive berry gel on loss of heterozygosity indices in premalignant oral lesions. *Clin. Cancer Res.*, **14**, 2421–2430.
4. Ugalde,C.M. *et al*. (2009) Distribution of anthocyanins delivered from a bioadhesive black raspberry gel following topical intraoral application in normal healthy volunteers. *Pharm. Res.*, **26**, 977–986.
5. Clifford,J.L. *et al*. (1999) Retinoid receptor-dependent and -independent effects of N-(4-hydroxyphenyl)retinamide in F9 embryonal carcinoma cells. *Cancer Res.*, **59**, 14–18.
6. Formelli,F. *et al*. (1996) Bioactivities of N-(4-hydroxyphenyl)retinamide and retinoyl beta-glucuronide. *FASEB J.*, **10**, 1014–1024.
7. Chiesa,F. *et al*. (2005) Randomized trial of fenretinide (4-HPR) to prevent recurrences, new localizations and carcinomas in patients operated on for oral leukoplakia: long-term results. *Int. J. Cancer*, **115**, 625–629.
8. Lippman,S.M. *et al*. (2006) Fenretinide activity in retinoid-resistant oral leukoplakia. *Clin. Cancer Res.*, **12**, 3109–3114.
9. William,W.N.Jr *et al*. (2009) High-dose fenretinide in oral leukoplakia. *Cancer Prev. Res. (Phila)*, **2**, 22–26.
10. Tradati,N. *et al*. (1994) Successful topical treatment of oral lichen planus and leukoplakias with fenretinide (4-HPR). *Cancer Lett.*, **76**, 109–111.
11. Mallery,S.R. *et al*. (2011) Effects of human oral mucosal tissue, saliva and oral microflora on intraoral metabolism and bioactivation of black raspberry anthocyanins. *Cancer Prev. Res. (Phila)*, **4**, 1209–1221.
12. Desai,K.G. *et al*. (2011) Development and *in vitro-in vivo* evaluation of fenretinide-loaded oral mucoadhesive patches for site-specific chemoprevention of oral cancer. *Pharm. Res.*, **28**, 2599–2609.
13. Vaishampayan,U. *et al*. (2005) Phase II trial of fenretinide in advanced renal carcinoma. *Invest. New Drugs*, **23**, 179–185.
14. Ren,F. *et al*. (2010) Quantitative proteomics identification of phosphoglycerate mutase 1 as a novel therapeutic target in hepatocellular carcinoma. *Mol. Cancer*, **9**, 81.
15. Halbert,C.L. *et al*. (1992) The E6 and E7 genes of human papillomavirus type 6 have weak immortalizing activity in human epithelial cells. *J. Virol.*, **66**, 2125–2134.
16. Illingworth,N.A. *et al*. (2010) Characterization of the metabolism of fenretinide by human liver microsomes, cytochrome P450 enzymes and UDP-glucuronosyltransferases. *Br. J. Pharmacol.*, **162**, 989–999.
17. Villani,M.G. *et al*. (2004) Identification of the fenretinide metabolite 4-oxo-fenretinide present in human plasma and formed in human ovarian carcinoma cells through induction of cytochrome P450 26A1. *Clin. Cancer Res.*, **10**, 6265–6275.
18. Abou-Issa,H. *et al*. (1997) Chemotherapeutic evaluation of N-(4-hydroxyphenyl)retainamide-O-glucuronide in the rat mammary tumor model. *Anticancer Res.*, **17**, 3335–3339.
19. Rinaldi,A.L. *et al*. (2002) Curcumin activates the aryl hydrocarbon receptor yet significantly inhibits (-)-benzo(a)pyrene-7R-trans-7,8-dihydrodiol bioactivation in oral squamous cell carcinoma and oral mucosa. *Cancer Res.*, **62**, 5451–5456.
20. Wu,X. *et al*. (2012) Mucoadhesive fenretinide patches for site-specific chemoprevention of oral cancer: enhancement of oral mucosal permeation of fenretinide by co-incorporation of propylene glycol and menthol. *Mol. Pharm.,* in press., doi: 10.1021/mp200655k
21. Lippens,S. *et al*. (2005) Death penalty for keratinocytes: apoptosis versus cornification. *Cell Death Differ.*, **12**, 1497–1508.
22. Candi,E. *et al*. (2005) The cornified envelope: a model of cell death in the skin. *Nat. Rev. Mol. Cell Biol.*, **6**, 328–340.
23. Lesort,M. *et al*. (1998) Distinct nuclear localization and activity of tissue transglutaminase. *J. Biol. Chem.*, **273**, 11991–11994.
24. Tatsukawa,H. *et al*. (2011) Dual induction of caspase 3- and transglutaminase-dependent apoptosis by acyclic retinoid in hepatocellular carcinoma cells. *Mol. Cancer*, **10**, 4.
25. Smith,J. *et al*. (2009) Biomarkers in dysplasia of the oral cavity: a systematic review. *Oral Oncol.*, **45**, 647–653.

Received November 22, 2011; revised February 16, 2012; accepted March 10, 2012